LAWRENCE
LIVERMORE
NATIONAL
LABORATORY

LLNL-JRNL-662724

Light Directed Electrophoretic Deposition for Additive Manufacturing:Spatially Localized Deposition Control with Photoconductive Counter Electrodes

A. J. Pascall, J. Mora, J. A. Jackson, J. D. Kuntz

October 16, 2014

Key Engineering Materials

Disclaimer

Light Directed Electrophoretic Deposition for Additive Manufacturing: Spatially Localized Deposition Control with Photoconductive Counter Electrodes

Andrew J. Pascall[1,a], Jeronimo Mora[1], Julie A. Jackson[1], and Joshua D. Kuntz[2]

[1]Engineering Directorate, Lawrence Livermore National Laboratory, 7000 East Avenue, Livermore, California, 94550, USA

[2]Physical and Life Sciences Directorate, Lawrence Livermore National Laboratory, 7000 East Avenue, Livermore, California, 94550, USA

[a]pascall1@llnl.gov

Keywords: Electrophoretic Deposition (EPD), Light Directed EPD, Additive Manufacturing, 3D printing, FEM Modeling, Simulations

Cite as: A. J. Pascall, J. Mora, J. A. Jackson, J. D. Kuntz, "Light Directed Electrophoretic Deposition for Additive Manufacturing: Spatially Localized Deposition Control with Photoconductive Counter Electrodes", Key Engineering Materials, Vol. 654, pp. 261-267, Jul. 2015. doi: 10.4028/www.scientific.net/KEM.654.261

Abstract. Electrophoretic deposition (EPD) has traditionally been viewed as a thin film deposition technique for coating conductive surfaces. Recently, there have been reports of producing functional parts with EPD to near net shape, often containing gradients in material properties normal to the conductive deposition surface. By using reconfigurable electrode systems, a few researchers have gone beyond purely out-of-plane gradients and demonstrated gradients in material properties in the plane of the deposition electrode, a necessary condition for 3D additive manufacturing. In this work, we build upon a previously published technique we developed called light directed electrophoretic deposition (LD-EPD) in which the deposition electrode is photoconductive and can be activated with light, leading to a patterned deposit. We demonstrate that the LD-EPD technique can also lead to patterned deposits on any conductive surface by utilizing the photoconductive electrode as the counter electrode. This eliminates several issues with standard LD-EPD by allowing the potentially expensive photoconductive electrode to be reused, as well as mitigates post-processing material compatibility issues by allowing deposition on any conductive surface. We also detail the results of a finite element simulation of the deposition process in LD-EPD systems that captures key features seen experimentally in the final deposit.

Introduction

Electrophoretic deposition (EPD), in which suspended colloids are deposited onto a surface with an electric field, has its origins in the early 20th century as a method for applying paint to conductive surfaces[1]. Consequently, the majority of work with EPD has focused on depositing conformal thin films on electrodes, albeit the electrodes may be of complex shape. There has been interest recently in extending EPD to produce functional parts to near net shape[2, 3].

Gradients in material properties can be built into parts by changing the composition of the deposition suspension during the course of the deposition[2, 4]. These gradients are typically limited to lie normal to the surface of the deposition electrode because material is deposited over the entire electrode surface layer by layer. Others have demonstrated in-plane control of deposits by lithographically patterning the deposition electrode, and thus the deposit[5, 6, 7]. However, due to the static nature of the patterned electrode, this method cannot be extended to form the thick, arbitrarily patterned deposits necessary for 3D additive manufacturing.

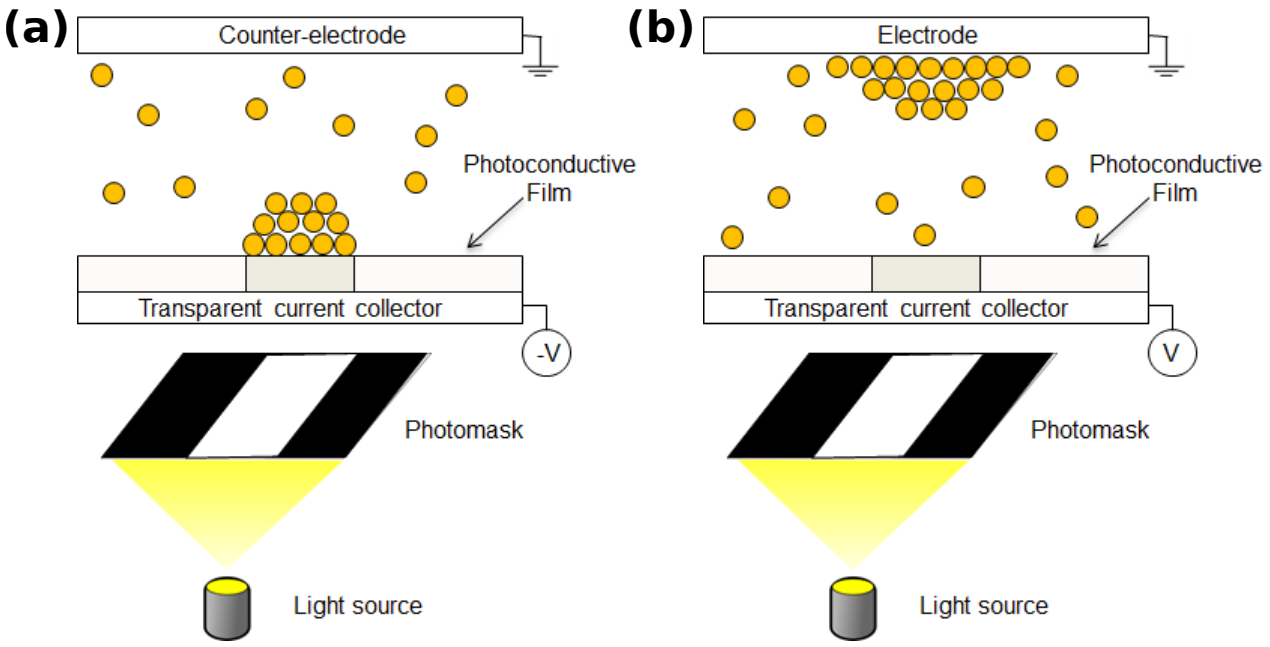

Fig. 1: (a) In the configuration presented in [10], the photoconductive electrode is utilized as the deposition electrode. This leads to the highest resolution deposition. (b) In this work, we pattern the photoconductive counter electrode which allows pattern transfer to the deposit on any deposition electrode, albeit with some degradation of resolution.

In order to utilize EPD as a 3D additive manufacturing technique, material must be deposited in localized regions on the electrode and those regions must be reconfigurable during the deposition, allowing gradients both in and out of the plane of the electrode. A series of papers by Nold, *et al.*[8, 9] demonstrated this by two methods: One utilized a coaxial electrode that was rastered over the surface of the deposition electrode. The other used a switchable 4x4 array of electrodes. They demonstrated the fabrication of millimeter scale features with a single material. Recently, Pascall, *et al.*[10] have developed light directed EPD (LD-EPD) in which a photoconductive electrode is patterned with light in order to activate the deposition electrode in specific areas, leading to high resolution features ($\sim$100 microns) with multiple materials (ceramic and metallic) deposited in specific locations.

In this work, we extend Pascall, *et al.*'s technique to allow for LD-EPD patterning of deposits on any conductive surface by utilizing the photoconductive electrode as the counter electrode (Fig. 1b). While the resolution will be limited compared to depositing directly on the photoconductive electrode due to fringing electric fields, there are several advantages: For instance, the photoconductive electrode is expensive, and it is desirable to reuse it. In some processes, the deposition electrode must be made of a specific material, so it is not possible to use a photoconductive electrode. Finally, we hypothesize that the feature resolution can be maintained over many layers as the counter electrode can be placed in close proximity to the growth front of the EPD film and translated with the growth of the film to maintain a set distance from the growth front. Here, we demonstrate a patterned deposited film on an unpatterned aluminum electrode produced by patterning the photoconductive counter electrode with UV light. We also detail the results of numerical modeling of patterned film deposition in LD-EPD in both the case when the photoconductive electrode is the deposition electrode as well as the case when it is the counter electrode.

Modeling

A finite element model of the LD-EPD process was constructed in COMSOL. The model is based on the one described in [11]. Namely, the time dependent governing equations are written for the

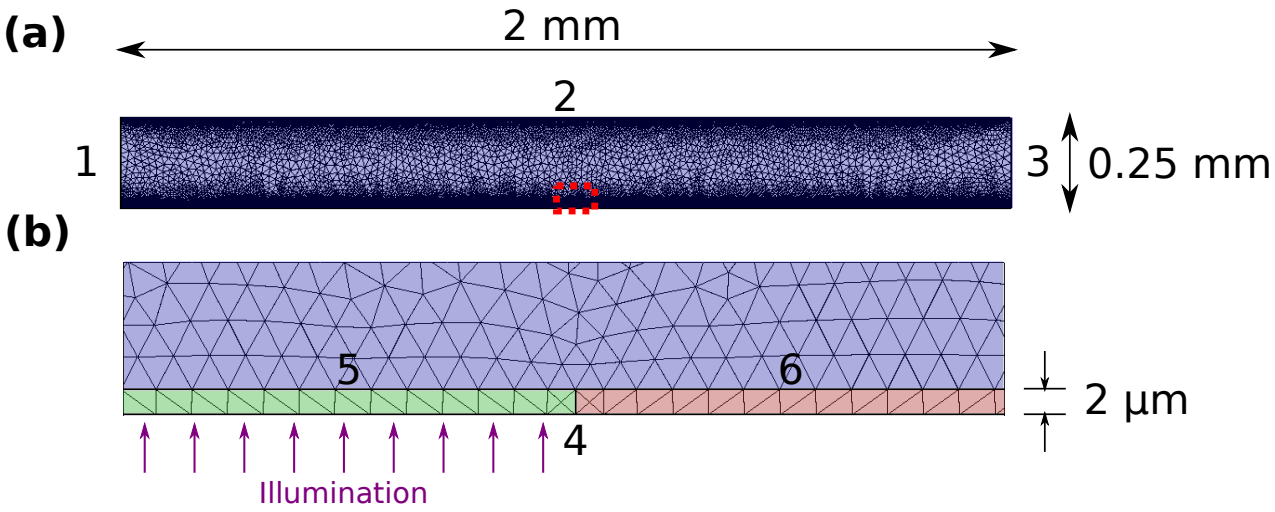

Fig. 2: (a) The deposition domain is shown with the mesh used in the finite element model. Boundaries 1 & 3 are assumed to be electrically insulating, while boundary 2 is set to ground potential, $\hat{V}$=0. (b) A zoomed in region corresponding to the red dashed box in (a). The blue domain represents the deposition region, while the green and red domains represent the illuminated and dark photoconductive regions, respectively. Boundary 4 represents the transparent current collector and its potential is set to $\hat{V}$=1 or -1, depending on if the photoconductive electrode is the deposition or counter electrode, respectively. On boundaries 5 and 6, there is continuity of electric current. The volume fraction boundary conditions are no flux on boundaries 1, 2, 3, 5, & 6. The mesh used in the calculations is represented by the array of triangles in the domain.

field variables, $\hat{V} = V/V_{\text{app}}$, which is the dimensionless electric potential in the domain, and the dimensionless volume fraction of particles, $\hat{\phi} = \phi/\phi_{\text{max}}$, where $\phi_{\text{max}} = 0.64$ represents the random close packed fraction:

$$\hat{\nabla}^2\hat{V} = 0\,, \tag{1}$$

$$\frac{d\hat{\phi}}{d\hat{t}} = \hat{\nabla}\cdot\left[\text{Pe}^{-1}\hat{\nabla}\hat{\phi} + \exp\left(-2.5\phi_{max}\frac{\hat{\phi}}{1-\hat{\phi}}\right)\hat{\phi}\hat{\nabla}V\right]\,, \tag{2}$$

where $\text{Pe} = 2\pi\varepsilon\zeta V_{app}d/k_BT$ is the Péclet number representing the relative significance of electrophoresis to diffusion in the movement of the particles, where ε is the solvent permittivity, ζ is the particle zeta potential, and d is particle diameter. $\hat{t} = t/t_c$ is the dimensionless time, with the characteristic time, t_c, chosen to be the time it takes a particle to move 100 microns by electrophoresis. The experimental value of Pe is calculated to be roughly 10^4; however, Pe = 10^3 was utilized in the simulation due to numerical stability issues with the COMSOL solver.

A detailed derivation of these equations can be found in [11]. The main difference between this model and the previously published model is the inclusion of the photocondutive layer and solving for the electric field using the ``Electric Currents'' module in COMSOL. The photoconductive layer is modeled as separate domains for both the illuminated and dark regions as described below: The first domain represents the suspension and deposition region which has dimensions 0.25 mm by 2 mm. This domain is represented by blue in Fig. 2, and has a relative permittivity of 24.3. Both $\hat{V}$ and $\hat{\phi}$ are calculated in this region. The second domain represents the illuminated region of the photoconductive film with dimensions 2 microns by 1 mm. This domain is represented by green in Fig. 2(b), and has a relative permittivity of 11.7 and conductivity relative to the solvent of 1×10^{-2}. The third domain represents the dark region of the photoconductive film with dimensions 2 microns by 1 mm. This domain is represented by red in Fig. 2(b),and has a relative permittivity of 11.7 and conductivity relative to the solvent of 1×10^{-3}. Only $\hat{V}$ is computed in this domain as it represents the solid

photoconductive film. The boundary condition applied between domain 1 and domains 2 and 3 is that the electrical current is continuous across the interface. The goal of the modeling is to qualitatively reproduce key features of actual LD-EPD deposits, therefore, the values of parameters for the model were chosen accordingly and may not represent actual values in the experiment.

Experimental

A 2 vol% copper suspension in ethanol was prepared as follows: 2.785 g copper nanopowder (Nanoamor, 0292HW) and 67 mg dopamine HCl (Sigma-Aldrich) were added to a scintillation vial. 11.873 g absolute ethanol was added and the suspension was mixed using an ultrasonic processor (Qsonica, 50% duty cycle, 3 seconds on per cycle, 1 minute total on time). After sonication, the particle size and zeta potential were measured to be 300 nm in diameter and 50 mV, respectively (ZetaSizer Nano Z90, Malvern).

The suspension was flowed into a custom built EPD cell as described in [10]. The electrodes were 25 mm x 25 mm, and the distance between electrodes was fixed at 250 microns by a Delrin spacer. The deposition electrode was a mill finish aluminum plate rinsed with ethanol and dried with nitrogen, while the counter electrode was a TiO_2 on FTO photoconductive electrode prepared by a previously published method [10].

Deposition was performed by first illuminating the backside of the photoconductive electrode with light from a 375 nm UV LED. Then, a voltage of 2 V_{DC} was applied between the deposition electrode and the current collector of the photoconductive electrode. After 1 hour, the voltage was decreased to 1 V_{DC} and the residual suspension was withdrawn at 0.25 mL/min.

Results and Discussion

The results of numerical modeling of LD-EPD are presented in Fig. 3. Fig. 3a shows the norm of the electric field in the domain. The electric field is the strongest at the boundary between the illuminated and dark regions. This is due to the electrical conductivity jump in the photoconductive layer. There is also significant field in the space between the illuminated electrode region and the counter electrode, while the field is lower between the dark electrode region and the counter electrode. This difference in electric field is the origin of the patterned deposit on the counter electrode.

Fig. 3b shows the deposited film when the photoconductive electrode is positively biased corresponding to the deposition mode depicted in Fig. 1a. It shows the hallmark feature of a thicker deposit at the boundary between illuminated and dark regions of the photoconductive electrode that was observed in [10]. Furthermore, it can be seen that a small amount of deposition is predicted to occur even over the dark region. This is due to the finite conductivity of the photoconductive film in the dark state. This creates a weak electric field which causes an thin EPD layer to form over the dark region. This can be mitigated by choosing a photoconductive film that shows a large difference between illuminated and dark conductivity. Here, we chose to model a factor of 10 difference in conductivity; however, factors of 10^9 have been reported for some photoconductors[12].

Fig. 3c shows the deposited film when the photoconductive electrode is negatively biased corresponding to the deposition mode depicted in Fig. 1b. It can be seen that the deposit is thickest above the illuminated region while there is a slightly thinner deposit over the dark region. The deposit in the dark region has two origins: First, as discussed above, there is a weak electric field in the dark region due to the finite conductivity of the dark state. This can be mitigated by choosing a photoconductor with the largest possible difference between light and dark conductivities. Second, the electric field fringes due to the large planar deposition electrode causing the field to spread over a larger area on the deposition electrode. This leads to a decrease in lateral resolution and can be mitigated by placing the counter electrode as close as to practical to the deposition front of the film. Indeed, it may even be advantageous to keep a small fixed distance between the deposition front and counter electrode

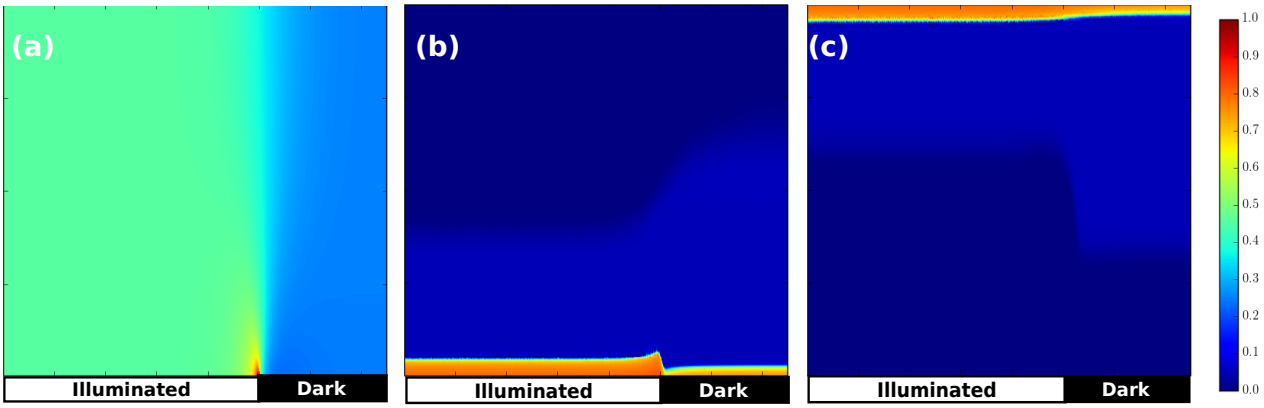

Fig. 3: (a) Norm of the electric field. The electric field is the strongest at the boundary between the illuminated and dark regions. This is due to the electrical conductivity jump between these regions. There is significant field in the space between the illuminated electrode region and the counter electrode, while the field is lower between the dark electrode region and the counter electrode. This difference in electric field is the origin of the patterned deposit on the counter electrode. (b & c) Represents the scaled volume fraction, $\hat{\phi}$, at a deposition time of $\hat{t} = 3$. High volume fractions (red) occur near the negatively biased electrode representing the deposit. (b) When the photoconductive electrode is negatively biased, a deposit (red region) is formed on the photoconductive electrode (Fig. 1a) due to the positive zeta potential of the suspension. Note that the deposit is thicker near the boundary between the illuminated and dark regions, as seen experimentally in [11, 10]. (c) When the photoconductive electrode is positively biased, a deposit is formed on the counter electrode (Fig. 1b). The deposit is thickest above the illuminated region while there is a slightly thinner deposit over the dark region. Colorbar represents $|\hat{E}|$ for (a) and $\hat{\phi}$ for (b & c). Note that the photoconductive electrode is at the bottom edge of all figures, and the counter electrode is along the top edge.

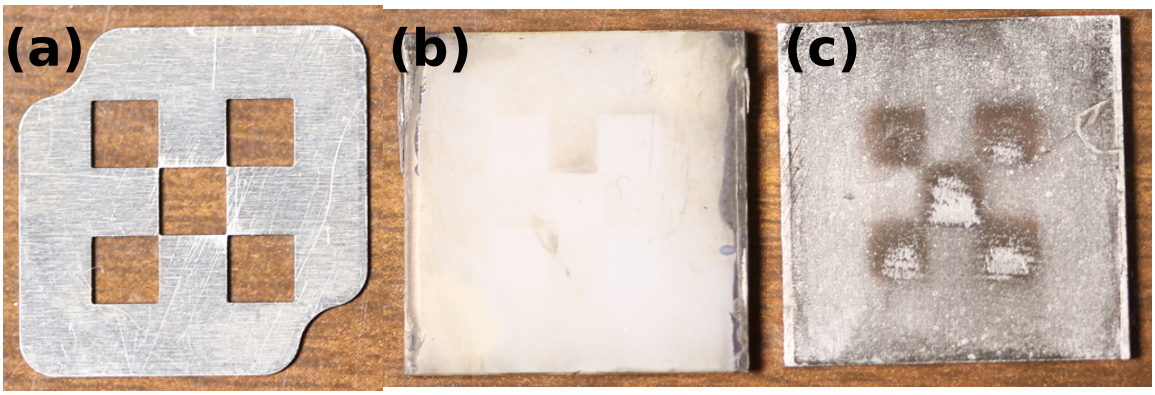

Fig. 4: (a) The laser cut anodized aluminum photomask. (b) Photoconductive counter electrode after deposition. (c) Patterned deposit of copper nanoparticles on aluminum deposition electrode. Note that the photomask pattern has been transferred to the deposit.

when depositing thick or 3D patterned films to maintain high resolution. This can be achieved by withdrawing the deposition electrode at the same rate as deposition.

Fig. 4 depicts the experimental realization of light directed EPD through photoconductive counter electrode patterning. Fig. 4a is the aluminum mask that is used to pattern the illumination for the photoconductive electrode. Fig. 4b shows the photoconductive counter electrode after production of the deposit, which is shown in Fig. 4c. The area corresponding the illuminated region is visibly cleaner than elsewhere on the counter electrode. We believe this is due to weakly adhered copper nanoparticles being transported away from the photoconductor via electrophoresis.

The patterned deposit on the aluminum electrode is clearly evident proving that the deposition scheme depicted in Fig. 1b is realizable in practice. It should be noted that the copper film was not very well adhered to the aluminum substrate and that regions of the film flaked off of the deposit during drying. These patches are evident as bright areas in the deposit region and are due to substrate handling and not to a fundamental limitation of the process. While the deposited film is much thicker in the regions corresponding to the regions illuminated on the photoconductive electrode, there is still some deposition evident in the dark regions for the reasons detailed above.

It should also be noted that the method of photoconductive counter electrode LD-EPD is quite general and is compatible with any suspension that can be electrophoretically deposited, regardless of optical density of suspension. This is because the illumination that actuates the counter electrode is performed through the transparent (glass) backside of the photoconductive electrode. Thus, light need not propagate through the suspension to yield patterning, only the patterned electric field is present.

Summary

We have shown that patterned EPD films can be deposited onto uniformally conductive electrodes by using a photoconductive counter electrode patterned with light. This work builds off our previously published work on LD-EPD onto photoconductive electrodes [10]. We have also constructed a finite element numerical model of LD-EPD that qualitatively reproduces many features evident in films deposited under both modes of LD-EPD.

This work adds versatility to the LD-EPD technique in that patterned deposits can be formed on any conductive electrode. This allows the photoconductive electrode, which is expensive and time consuming to fabricate, to be reused. It also removes processing constraints by allowing deposition on electrodes that are optimized for the material system deposition. Finally, it may allow high resolution 3D patterning of thick films, which is desirable for 3D additive manufacturing.

Acknowledgments

This work was funded by the Laboratory Directed Research and Development Strategic Initiative program 14-SI-004 and performed under the auspices of the US Department of Energy by Lawrence Livermore National Laboratory under Contract DE-AC52-07NA27344. LLNL-JRNL-662724.

References

[1] W. P. Davey, February 1919. United States Patent 1,294,627.

[2] G. Anné, K. Vanmeensel, J. Vleugels, and O. Van der Biest. *Key Eng. Mater.*, 314:213--218, 2006.

[3] C. Oetzel and R. Clasen. *J. Mater. Sci.*, 41(24):8130--8137, November 2006.

[4] H. Hadraba, D. Drdlik, Z. Chlup, K. Maca, I. Dlouhy, and J. Cihlar. *J. Eur. Ceram. Soc.*, 33(12):2305--2312, October 2013.

[5] S. Ahmed and K. M. Ryan. *Adv. Mater.*, 20(24):4745--4750, December 2008.

[6] A. J. Krejci, J. Mandal, and J. H. Dickerson. *Applied Physics Letters*, 101(4):043117-4, July 2012.

[7] F. Qian, A. J. Pascall, M. Bora, T. Y. Han, S. Guo, S. Ly, M. A. Worsley, J. D. Kuntz, and T. Y. Olson. *Langmuir*, doi:10.1021/la502724n, September 2014.

[8] A. Nold, T. Assion, J. Zeiner, and R. Clasen. *Key Eng. Mater.*, 412:307--312, 2009.

[9] A. Nold, J. Zeiner, T. Assion, and R. Clasen. *J. Eur. Ceram. Soc.*, 30(5):1163--1170, March 2010.

[10] A. J. Pascall, F. Qian, G. Wang, M. A. Worsley, Y. Li, and J. D. Kuntz. *Adv. Mater.*, 26(14):2252--2256, April 2014.

[11] A. J. Pascall, K. T. Sullivan, and J. D. Kuntz. *J. Phys. Chem. B*, 117(6):1702--1707, February 2013.

[12] N. M. Phuong, N. Seong, J. Ahn, E. Kim, J. Lee, G. H. Kim, and S. Yoon. *Electrochem. Solid-State Lett.*, 10(9):H284--H286, 2007.